Hybrid PMMA combined with polycarbonate inside interpenetrating polymer network architecture for development of new anti-scratch glass

Isabelle Fabre-Francke, Mickaël Berrebi, Bertrand Lavédrine, Odile Fichet

Hybrid PMMA combined with Polycarbonate inside interpenetrating polymer network architecture for development of new anti-scratch glass

Isabelle Fabre-Francke[a], Mickaël Berrebi[a,b] Bertrand Lavédrine[b], Odile Fichet[a*]

[a] Laboratoire de Physicochimie des Polymères et des Interfaces (LPPI) - Institut des Matériaux, Université de Cergy-Pontoise, 5 mail Gay-Lussac Neuville-sur-Oise, 95031 Cergy-Pontoise Cedex, France

[b] Centre de Recherche sur la Conservation des Collections (CRCC), Muséum National d'Histoire Naturelle, Ministère de la Culture et de la Communication, USR CNRS 3224, 36 rue Geoffroy St Hilaire, 75005 Paris, France

*Corresponding author. Tel.: +33-1-34-25-70-50; fax: +33-1-34-25-70-71.

Email address: odile.fichet@u-cergy.fr

Abstract

Polymethyl methacrylate (PMMA) is commonly used as organic glass for the protection of works in museums. However, their extreme sensitivity to scratching causes problems during maintenance procedures. In order to improve the resistance to abrasion, PMMA has been cross-linked with silica nanoparticles previously modified with 3-(methacryloxy)propyl-trimethoxysilane (MPTS). This functionalization allows both a homogeneous dispersion of the silica nanoparticles in MMA monomer and the PMMA crosslinking which has been confirmed by solid/liquid extraction and DMA analysis. The small nanoparticles (7 - 10 nm diameter) added in different amounts, are homogeneously dispersed in the transparent (T% > 80%) hybrid $PMMA_x$-SiO_2 networks as verified by TGA and TEM microscopy. These hybrid $PMMA_x$-SiO_2

networks have been then combined with a PCR39® polycarbonate network in an interpenetrating polymer network (IPN) architecture. The synthesis of a hybrid IPN in which one of the phases is cross-linked by the inorganic nanoparticles has been demonstrated for the first time. Finally, as expected, the incorporation of the silica nanoparticles improves the scratch resistance by a factor of 3 compared to all organic PMMA/PCR39® IPNs.

Keywords: Polycarbonate, Polymethyl methacrylate, Hybrid interpenetrating polymer networks (hybrid IPNs), anti-scratch properties.

1. Introduction

Polymethyl methacrylate (PMMA) is used in numerous applications because of its optical properties close to those of glass. Indeed, the refractive indices of PMMA and glass are of 1.491 [1] and 1.522 [2], respectively. PMMA also exhibits a better light transmission, is significantly (1.19 $g.cm^{-3}$ by respect to 2.5 $g.cm^{-3}$) and less brittle than glass. However, PMMA exhibits poor resistance to scratching [3-4] .

To enhance the PMMA's scratch resistance, it was combined with polycarbonate (PCR39®) in interpenetrating polymer network (IPN) architecture. An IPN is defined as a combination of at least two cross-linked polymers, one of being synthesized in the presence of the other [5]. Thus, a series of transparent IPNs (transmission higher than 95%) based on the combination of an aliphatic polycarbonate PCR39® and PMMA was synthesized without solvent according to in situ polymerizations [6]. The scratch tests revealed that the addition of only 25 wt% PCR39® in PMMA network is sufficient to improve the PMMA's scratch resistance.

An alternative route to improve scratch resistance of polymer material is based on the incorporation of inorganic compounds. For instance, Bauer et al. [7] have studied the effect of nanoparticles functionalized by a trialkoxysilane with a terminal vinyl function on the anti-abrasive properties of a polyacrylate-based UV topcoat for parquet (SR-494/PHEMA). Authors have shown that abrasion is significantly more decreased with the introduction of functionalized alumina, silica or zirconium than that of modified titanium nanoparticles. The key role of the functionalization of nanoparticles (30-40 nm diameter) on the abrasion resistance has also been confirmed by the same authors on the coating of SR 494. Indeed, the SR 494 topcoat containing 35 wt% nanoparticles functionalized with 3-(methacryloxy)propyl-trimethoxysilane (MPTS) is 4 times more scratch resistant than the coating alone in which less than 15 wt% unmodified silica can be included [8-9].

The aim of our research project is focused on the development of a hybrid interpenetrating polymer network based on organic PMMA/PCR39® IPN. The first challenge is generally the control of the homogeneous dispersion of the filler within the polymer matrix. Thus, silica *in situ* synthesized from tetraethoxysilane or trimethoxysilane is used almost exclusively as inorganic phase [10-11]. In this work, exogenous silica nanoparticles have been selected because of their capability to be dispersed in both PMMA-based and polycarbonate-based materials.

The main objectives of the nanoparticle addition in PMMA generally is to increase its glass transition temperature (Tg), its mechanical modulus and/or its thermal resistance. For instance, PMMA's Tg is increased from 106°C to 122°C when TiO_2 nanofibers modified with methacrylic acid are incorporated from 0 wt% to 17 wt% [12]. However, when the fillers are not functionalized, the Young's modulus is decreased

and Tg does not evolve steady. This suggests the importance of the functionalization of the inorganic fillers for their integration within PMMA materials. Furthermore, Otsuka et al. [13] have functionalized 5 nm zirconium oxide nanoparticles with MPTS in order to disperse them in methylmethacrylate (MMA) monomer. The authors show that the incorporation of up to 39 wt% ZnO_2 functionalized nanoparticles leads to the preparation of transparent PMMA networks with improved thermal resistance (degradation temperature - Td=280°C) compared to uncharged PMMA (Td=200°C). Silica is also often used as nanoparticles. They were previously modified with allyl glycidyl ether [14] or with 3-methacryloxypropyl dimethylchlorosilane [15], for example. Thus, the synthesis of hybrid PMMA network was carried out with from 10 to 23 wt% of 20 nm silica nanoparticles modified with 3-methacryloxypropyl dimethylchlorosilane by quasi-living polymerization. No nanoparticle aggregation was observed and the PMMA mechanical relaxation temperature $T\alpha$ was risen by approximately 10°C. Simultaneously a slight increase in storage and loss moduli of the rubber plateau was detected. These results therefore indicate that PMMA was crosslinked by the silica nanoparticles under these conditions. While hybrid material based on PMMA are widely described, few of these studies care about PMMA scratch resistance. On the one hand, Avella et al. [16] have shown that the PMMA's anti-abrasive properties are improved (a weight loss two times less was measured for a similar abrasion) when 6wt% $CaCO_3$ nanoparticles (about 40 nm diameter functionalized with stearic acid) are added. On the other hand, Rodriguez et al. [17] have inserted up to 30 wt% silica nanoparticles functionalized with dichlorodimethylsilane in PMMA. They show that 50 µm coating spread on wood reduces by four the weight loss during abrasion compared to that of the commercial coating (name and composition not specified). However, in

this case, nanoparticles are not grafted on PMMA and can thus migrate in organic matrix over time.

Polycarbonate (PC) has also been studied as organic matrix of hybrid materials. For instance, it has been associated with zinc oxide nanoparticles to improve its wear resistance [18]. The introduction of only 0.5 wt% of non-functionalized nanoparticles increases its hardness and thus the hybrid material wear during an abrasion test is lower than that of pure PC. However, the material heterogeneity simultaneously leads to the decrease of thermal stability. In addition, the incorporation of ZnO nanoparticles in polycarbonate matrix increases the material brittleness at room temperature by a factor of 2.72 [19]. Other nanoparticles such as $CaCO_3$ or aluminum nanofibers were introduced in polycarbonate to improve its mechanical properties. However, a transparency loss was observed beyond 0.5 wt% fillers (transmission at 450 nm less than 80%) due to the charge's agglomeration [20-21]. All these results highlight either a loss of transparency or a degradation of the mechanical or thermal properties of filled PC. The effect of the introduction of silica nanoparticles on the polycarbonate scratch resistance was also studied by coating but not in bulk. For that, a mixture of polycarbonate with 20 wt% silica was deposited on the PC surface and covalent bonds are created between the polymer and the fillers by a sol-gel process method [22]. The depth of scratches was less important when the PC is previously modified with a PC-SiO_2 coating whatever its thickness rather than a single PC film. In addition, this PC-SiO_2 coating induces an increase in the hardness, the elastic modulus as well as the scratch recovery capability.

Hybrid organic–inorganic UV-cured coatings based on interpenetrating polymer networks were finally synthetized from bisphenol-A-diglycidyl ether dimethacrylate /

diglycidyl ether of bisphenol A in the presence of 15wt% fumed silica nanoparticles [23]. An improvement of 34% of compression strenght was obtained for (50/50) hybrid IPNs.

As the nanoparticle dispersion seems easier in PMMA than in polycarbonate, we focused our work on the development of a series of hybrid PMMA/PCR39® IPNs in which PMMA would be cross-linked by silica nanoparticles. For that, the surface of the silica nanoparticles has been first functionalized with methacrylate functions to help their copolymerization with MMA monomers. Hybrid PMMA networks were then first synthesized and characterized. These hybrid networks were included in IPN architecture with PCR39® polycarbonate to obtain homogeneous transparent materials with a scratch resistance higher than those of corresponding organic materials were.

2. Experimental Section

2.1. Materials

Diethylene glycol bis-allyl carbonate (CR39®) (Aldrich), methyl methacrylate (MMA) (Acros organics 99%), dicyclohexyl peroxidicarbonate (DCPD) (group Arnaud), 3-(methacryloxy)propyl-trimethoxysilane (MPTS) (ABCR), methanol (VWR) and dichloromethane (GPR Rectapur® VWR) were used as received. SiO_2 nanoparticles of 4.1±1.3 nm diameter were furnished (ABCR) in pH 10.0 aqueous solution at 15%wt SiO_2 concentration. Benzoyl peroxide (BPO) (Aldrich 75%) was dried under vacuum at room temperature for 24h before use.

2.2. Preparation of MPTS-modified SiO_2 as cross-linker

The functionalization of SiO_2 nanoparticles was carried out with 6.67g of SiO_2 aqueous solution (1g SiO_2) in which from 0.12 to 0.35g MPTS (according to the expected grafting ratio) and 20 mL methanol were added. The molar ratio between MPTS and silica nanoparticles was thus between 50 and 150. The transparent methanol/water solution was then shaken under 130 W ultrasonic bath for 10 min and heated at reflux with vigorous stirring for 15h. Methanol was then removed with a vacuum rotary evaporator and a thick and white solution was obtained. For the nanoparticle characterizations, this solution was dried at 90°C for 1h to remove residual methanol and MPST (less than 2% determined by TGA).

For the material synthesis, the previous solution was extracted with 0.8 equivalent weight of MMA in which MPTS-modified SiO_2 nanoparticles spontaneously migrate. Thus, a MMA solution containing 1% nanoparticles (determined by TGA measurements) was obtained. To increase the proportion of functionalized nanoparticles, the solution was concentrated with a rotary evaporator from 1 to 13 wt% (also determined by TGA measurement). When the proportion becomes higher than 13wt%, the MMA solution clouded.

2.3. Synthesis of hybrid PMMAx-SiO_2 network

Single PMMA networks were synthesized starting from the previous MMA solutions containing different proportions of MPTS-modified SiO_2. They were prepared by mixing 1g MPTS-modified SiO_2/MMA solution and 5mg (30 µmol) DCPD free radical initiator (0.5 wt% with respect to MMA). The mixture was degassed under argon and then poured into the mould made from two glass plates clamped together and sealed with 1mm thick Teflon® gasket. The mould was then kept at 35°C for 3h and post-cured at 80°C for 1h. Rigid transparent materials were obtained. They are noted $PMMA_x$ in the

text where x is the nanoparticle weight proportion in the precursor MMA solution. All synthesized materials are transparent.

2.4. Synthesis of hybrid $PMMA_x$-SiO_2 / PCR39® IPNs

Hybrid $PMMA_{13}$-SiO_2 / PCR39® (50/50) IPN was synthesized as follows: 0.5g of MMA solution containing 13 wt% MPTS-modified SiO_2 was mixed with 0.5g (1.8mmol) CR39®. Then 2.5mg DCPD (15µmol - 0.5 wt% with respect to MMA) and 25mg BPO (0.1mmol - 5 wt% with respect to CR39®) were added. The solution was degassed under argon and then poured into the mould previously described. The mould was heated in an oven at 35°C for 3h, at 80°C for 2h and 100°C for 1h. After mould removal, hybrid $PMMA_{13}$-SiO_2 / PCR39® (50/50) IPN is transparent.

IPNs with different PCR39® network contents ranging from 25 to 75wt% were synthesized keeping the same proportions between BPO initiator and CR39® (5 wt% BPO) and between DCPD initiator and MMA (0.5 wt%). Whatever their composition, all synthesized IPNs are transparent.

2.5. Synthesis of semi $PMMA_x$ / PCR39® IPNs

Semi PMMA / PCR39® IPNs were synthesized under the same conditions as corresponding hybrid $PMMA_x$-SiO_2 / PCR39® IPNs except MMA solution with nanoparticles was replaced by pure MMA.

2.6. Polymerization and polycondensation of MPTS

MPTS radical polymerization was carried out by adding 5mg DCPD (0.5 wt% with respect to the MPTS) to 1g MPTS. The mixture was degassed 15 min under argon and

then inserted into a test tube. The thermal program was applied from 3h to 35°C and then from 1h to 80°C.

PolyMPTS was formed by hydrolysis reaction followed by condensation of the methoxy functions of MPTS. For that, 1g MPTS in 20 mL methanol were placed in a flask and heated at reflux with vigorous stirring for 15h. Then, methanol was removed with a rotary evaporator.

2.7. Characterizations

Nanoparticle size distribution was determined in colloid solution with Zetasizer NanoS PCS (Photon Correlation Spectroscopy) from Malvern Instrument at 25°C.

In order to check the network formations, single networks, semi-IPNs and IPNs were extracted in a Soxhlet with dichloromethane for 72 h. After extraction, the sample was dried under vacuum and then weighted. The extracted content (EC) was given as a weight percentage (Eq.1.):

$$EC=\frac{(w_0-w_E)}{w_0}\times 100 \qquad \text{Equation 1.}$$

where W_O and W_E are the weights of samples before and after extraction, respectively. Each extraction was performed three times and the average value was given. The soluble fractions were then analyzed by ^{1}H NMR using the Brüker Avance DPX250.

The molecular weight between crosslinks (Mc) was measured by swelling the PMMAx-SiO_2 networks with dichloromethane. The networks were immersed up to have a constant mass. The uptake was calculated as (Eq.2.):

$$Uptake(\%)=\frac{(w_{after}-w_{before})}{w_{before}}\times 100 \text{ Equation 2.}$$

where w_{before} and w_{after} are the sample weights before and after immersion.

Thermogravimetric analyses (TGA) were performed on a Q50 model (TA Instruments) under synthetic air (60mL.min^{-1}) from room temperature to 700°C at 20°C.min^{-1} heating rate.

Dynamic thermomechanical analysis (DMA) measurements were carried out with a Q800 apparatus (TA instruments) operating in tension mode. Experiments were performed at a frequency of 1Hz and heating rate of 25°C.min^{-1} from 25 to 200°C. Typical dimensions of the samples were 8 mm X 20 mm X 1 mm. The damping parameter or loss factor is defined as tan $\delta = E''/E'$.

UV-visible spectra were recorded in absorbance mode with a JASCO V-570 spectrophotometer. The scan rate was set at 400 nm.min^{-1} between 250 and 800 nm. The thickness of the samples was about 250 μm or 1 mm.

Fourier transform infrared (FTIR) spectra were obtained using a Brüker spectrometer (Equinox 55) in the range 4000-500 cm^{-1} by averaging of 16 consecutive scans with a 2 cm^{-1}resolution.

Transmission electron microscopy (TEM) was performed with a Hitachi H-800 at 200 KV with a resolution of 0.2 nm on ultrafine cuts (about 40 nm thickness) of the samples. The contrast between the organic and inorganic phases was enhanced by the inorganic phase stained with osmium tetroxide.

The scratch tests were performed on a Scratch Hardness Tester Erichsen model 291. The pencil (8H hardness-grade - ISO 15184) was moved scratching over the surface

under a 45° angle with a 7.5N pressure. The scratch depth was measured with a Veeco Dektak 150 profilometer.

2.8. Artificial UV ageing

The artificial UV ageing of the samples was carried out in a Xenotest 220/220 + ageing chamber (ATLAS) equipped with a Xenon lamp equipped with a Xenochrome 320 filter to reproduce the solar spectrum behind a 3-mm thick glass window. The samples were placed in this climatic chamber at 50% RH, 25°C and irradiated at 50 $W.m^{-2}$ up to 548 hours. The samples were characterized before and after aging by UV-visible spectrometry.

3. Results and discussion

3.1. Characterizations of MPTS-modified SiO_2 nanoparticles:

First, the hydroxyl density on the surface of SiO_2 nanoparticles has been quantified by thermogravimetric analysis from loss weight starting from 120°C due to their deterioration [24]. A value of 2.4 $OH.nm^{-2}$ was obtained and it is consistent with values generally reported in literature (between 2 and 5 $OH.nm^{-2}$) [24-25]. Surface of these SiO_2 nanoparticles was then modified with various MPTS molar ratios (R = MPTS / SiO_2 nanoparticle = 50, 75, 100 and 150 – from 0.48 to 1.44 mmol MPTS) in a water / methanol (5/20 (v/v)) mixture. The obtained colloidal solution was heated at reflux for 15h and the solution becomes cloudy. After methanol evaporation, a viscous white solution was obtained (Figure 1). The modified nanoparticles were dried at 90°C for 1 h in order to eliminate water and residual MPTS before analysis. FT-IR analysis shows that the C-H stretching vibrations of MPTS methoxy groups at 2841 cm^{-1} have

disappeared proving that the hydrolysis of these functions is complete whatever the R ratio. In addition, the intensities of the specific bands of stretching modes of carbonyl C=O at 1717 cm^{-1} and of methacrylate C=C at 1637 cm^{-1} can be compared by normalizing the different spectra with the absorption band at 1100 cm^{-1} characteristic of Si-O-Si vibrations. Whatever the R values, the ratio of the C=O and C=C band areas is constant at about 0.2, the same value of that measured on polycondensed PMPTS. These analyses show that the MPTS methacrylate function does not polymerize during the SiO_2 nanoparticle modification.

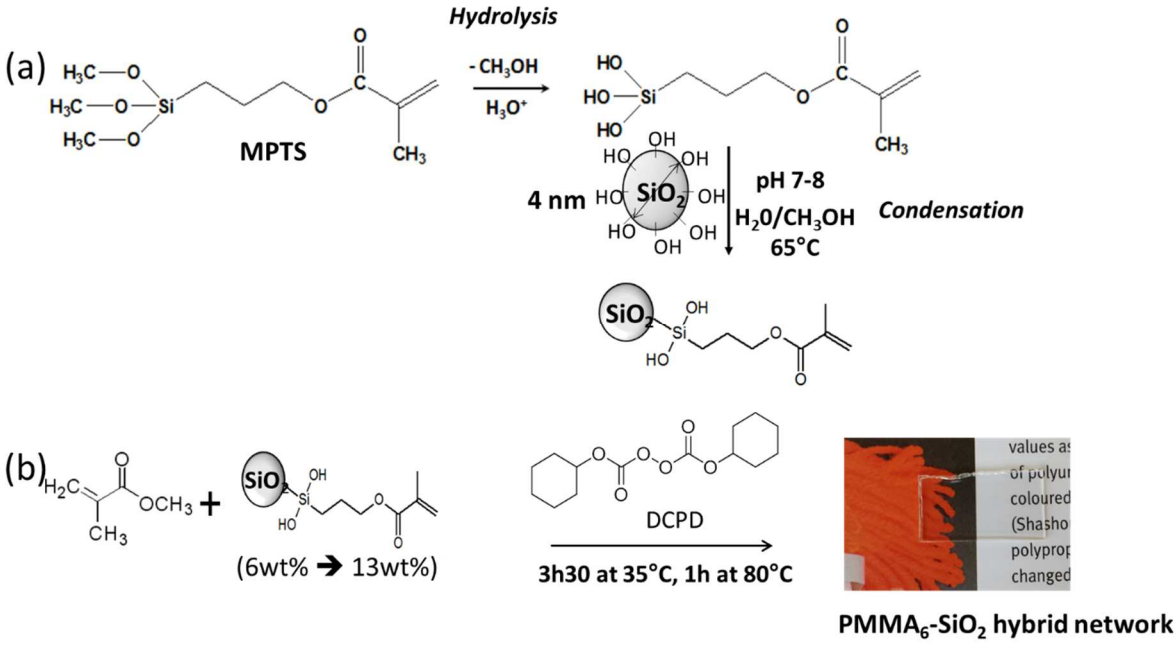

Fig. 1. Reaction pathway for (a) modification of SiO_2 nanoparticles with 3-(methacryloxy)propyl-trimethoxysilane (MPTS) then noted as MPTS-modified SiO_2 and (b) hybrid PMMAx-SiO_2 network.

To confirm that MPTS is grafted to the nanoparticles surface as expected, both polymers have been synthetized from MPTS solution in the absence of nanoparticle

and they have been characterized by TGA analysis. A first polymer (PMPTS) results of the free-radical polymerization of the MPTS methacrylate functions initiated by DCPD. A second polymer (PolyMPTS) is obtained from the condensation of the MPTS silanol functions which occurs after the hydrolysis of methoxy group. A 5% weight loss is measured by TGA analysis at 230°C for PolyMPTS and at 175°C for PMPTS (Fig.2.). In addition, methoxy function are not hydrolysed in PMPTS and they can be thus degraded by the temperature increase: the residual weight is thus close to zero. In contrast, the MPTS silanol functions resulting of the hydrolysis of methoxy group are transformed in silica after polycondensation. This silica cannot be thermally degraded, and the residual weight differs from zero. The thermal behavior of these organic MPTS-based materials is significantly different of that synthesized in the presence of SiO_2 nanoparticles which is stable up to 320°C (Fig.2.). Thus, MPTS seems preferentially to condense on the nanoparticle surface rather than in homopolymer form in the solution under the used experimental conditions.

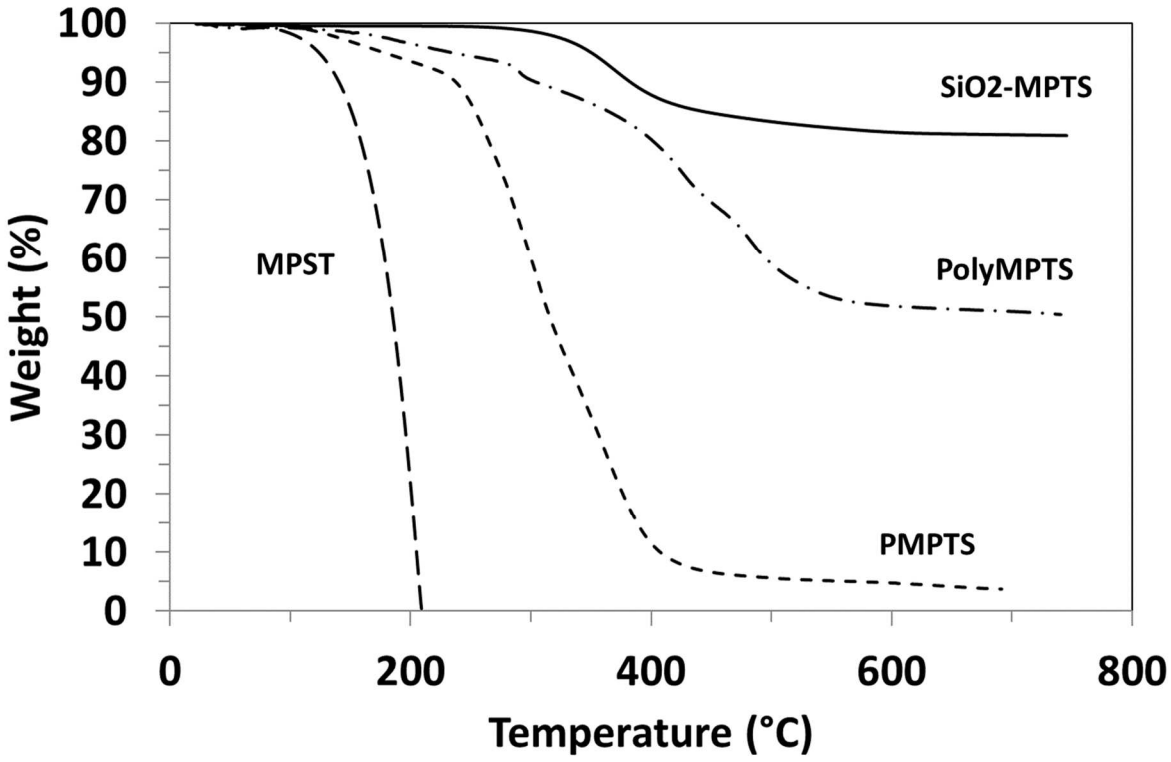

Fig.2. Thermogravimetric analysis (TGA) of (— —) MPTS, (---) PMPTS, (-·-) PolyMPTS and (—) MPTS-SiO_2 nanoparticles. Synthetic air flux: 60mL.min^{-1} - Heating rate: 20°C.min^{-1}

Effect of MPTS / SiO_2 nanoparticle molar ratio (R = 50, 75, 100 and 150) on the MPTS grafting ratio - defined as the ratio of grafted MPTS and MPTS used for the synthesis - was then evaluated (Table 1). The grafting ratio was determined from the weight loss (Supporting information – Fig.S1.) and calculated as [26] (Eq.3.):

$$Grafting\ ratio = \frac{\left(\frac{W_{\Delta T}}{100 - W_{\Delta T}}\right) \times 100 - W_{SiO2}}{M \times S_{spe} \times 100} \times 10^6$$

where $W_{\Delta T}$ is the weight loss at 750°C, M the molar weight of grafted-MPTS, S_{spe} the specific surface, and W_{SiO2} the weight loss of unmodified nanoparticles, respectively.

Since W_{SiO2} is very low (less than 2%), $W_{\Delta T}$ can be considered as coming only from the thermal degradation of the grafted MPTS on the nanoparticles.

MPTS / SiO_2 nanoparticle (R)	50	75	100	150
MPTS grafting ratio (%)	92	91	83	79
Theorical grafting degree (%)*	100	100	100	80
Molecular area by MPTS (nm^2)	1.15	0.77	0.64	0.45
Diameter of MPTS** (nm)	1.21	0.99	0.90	0.75
Modified nanoparticle diameter (nm)	8.7±2.4	10±2.4	6.7±2	10.1±2.4

** Calculated assuming a density of 120 OH by nanoparticle - ** Assuming a circle of projection*

Table 1. Characteristic of SiO_2 nanoparticles modified with different R molar ratios

$W_{\Delta T}$ increases from 12 to 26% when the R molar ratio increases from 50 to 150. However, in view of the introduced MPST amount, the MPTS grafting ratio decreases from 92 to 79% when R increases. These experimental values are close to the theoretical grafting ratios that shows that most OH functions on the nanoparticle surface have been modified by MPTS. From these measurements, it is also possible to estimate the molecular area of MPTS at the nanoparticle surface (Table 1), and to

deduce the diameter of the MPTS's projection surface (assumed to a disk) which varies from 1.2 to 0.75 nm.

Second, for the material synthesis, the MPTS-modified SiO_2 nanoparticles have been extracted from the aqueous solution with MMA. Whereas a sedimentation is always observed with unmodified nanoparticles, the extraction of modified nanoparticles with MMA is spontaneous and the resulting MMA solution is transparent. In order to verify the dispersion, a dynamic light scattering (DLS) analysis was performed on 1 wt% MPTS-SiO_2 nanoparticles in MMA solution. The nanoparticle diameter is 7-10 nm whatever the R ratio (Table 1) while the initial size of nanoparticles is 4 nm. The increase would correspond to a MPTS shell of about 1.5 to 3 nm thick in agreement with the MPTS length estimated to 1.1 nm and in agreement with previous results reported in the literature [27]. However, the MPTS's high is significantly higher that the diameter of the occupied surface by MPTS. Thus, it seems that MPST adopt rather a brush conformation at the surface of silica nanoparticles.

It was also checked by DLS analysis that the MPTS-SiO_2 nanoparticles remain stable at 25°C in MMA at least 3 h, time required for the PMMA network synthesis. It is thus possible to control the size and dispersion of MPTS-SiO_2 nanoparticles in MMA solution, a required condition for synthesis of transparent glass. For next work, silica nanoparticles were modified with a MPTS / SiO_2 nanoparticles ratio of R = 100.

3.2. Synthesis and Characterization of hybrid PMMAx-SiO_2 network: PMMAx-SiO_2 hybrid networks have been synthesized by free-radical polymerization of MMA monomer in the presence of 0.5%wt DCPD initiator and different weight proportions of

MPTS-SiO_2 nanoparticles (2-13.5%) as crosslinker (Fig.1.). After mixture of precursors, a thermal program of 35°C for 3h and a post-cured at 80°C for 1h was applied. Transparent materials were obtained.

First, the PMMA's crosslinking and the nanoparticles dispersion were analyzed. To show evidence of the cross-linking, the soluble fractions contained in the different single PMMAx-SiO_2 hybrid networks have been quantified by Soxhlet extraction (Fig.3.).

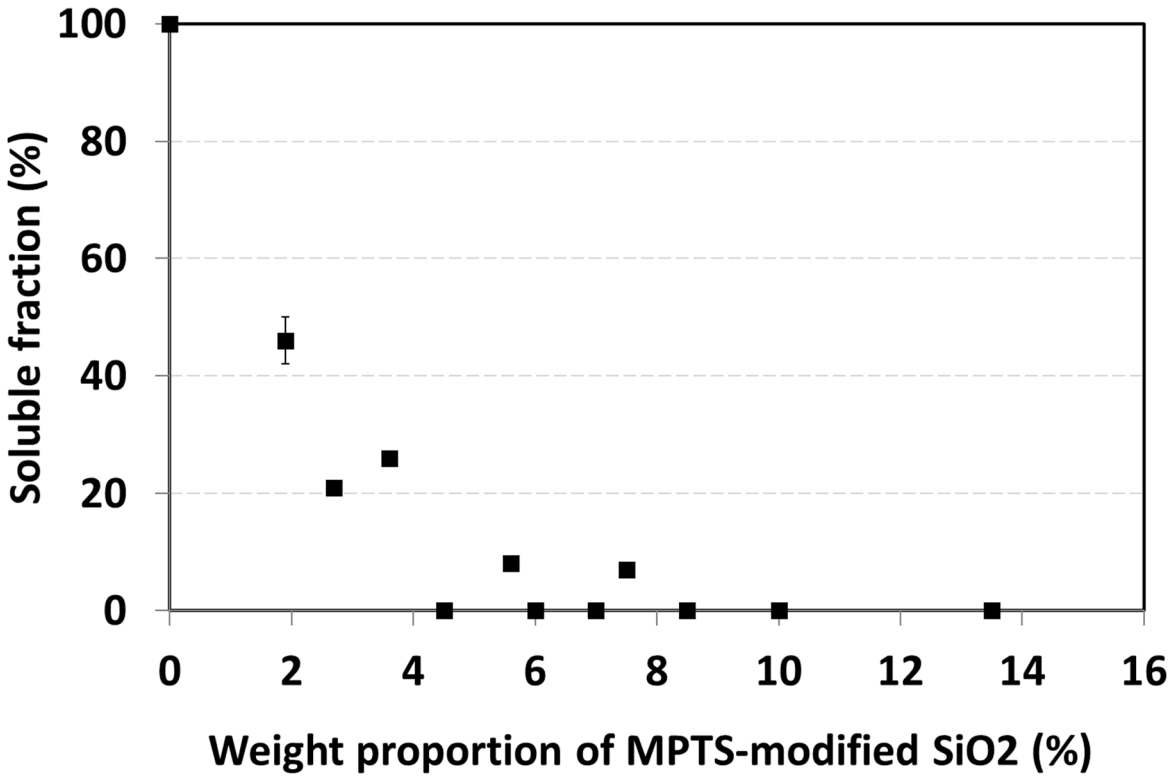

Fig.3. Soluble fraction contained in PMMAx-SiO_2 hybrid networks versus the weight proportion of MPTS-modified SiO_2 nanoparticles.

While the PMMA synthesized in the presence of unmodified nanoparticules is totally soluble in CH_2Cl_2, the soluble fractions contained in the materials decreases from 45

to 20 wt% when the MPTS-SiO_2 nanoparticle proportion increases from 2 to 4wt%. For nanoparticle proportions greater than 4 wt%, the PMMA's cross-linking is correct since the soluble fractions are near zero. As expected, the MPTS-modified SiO_2 nanoparticles act well as PMMA's crosslinkers. For the next experiments, only materials crosslinked with more than 4.5 wt% nanoparticles have been characterized.

All hybrid PMMAx-SiO_2 networks with x between 4.5 and 13.5 wt% are transparent, i.e. they exhibit a transmission value equal to 90% between 800 and 400 nm. In contrast, opaque materials were obtained with unmodified SiO_2 nanoparticles. The homogeneity of the modified nanoparticle distribution inside the PMMA networks was characterized on $PMMA_6$-SiO_2 network by TGA analysis of samples taken at various locations of the material. The nanoparticle amount ranges from 5.7 to 6.4% between the up and down of the material. No significant sedimentation was thus detected. The homogeneity of hybrid PMMAx-SiO_2 network was also confirmed by TEM analysis (Fig.4a.).

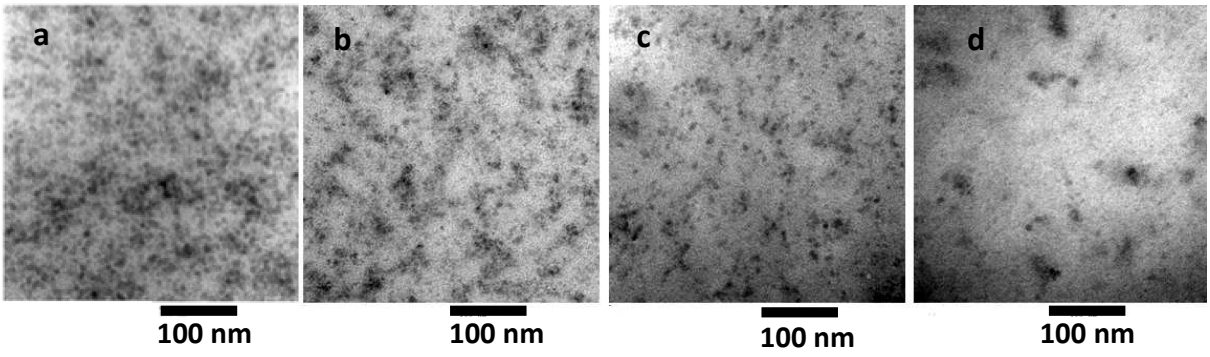

Fig.4. Transmission electron microscopy images of hybrid $PMMA_7$-SiO_2 network (X 257 000) (a), hybrid $PMMA_7$-SiO_2 /PCR39® IPNs (75/25) (b), (50/50) (c) and (25/75) (d) (X 171 000).

Well dispersed MPTS-modified SiO_2 particles (in black) were observed in the PMMA matrix. In addition, they are not aggregated since the nanoparticle sizes estimated from this image is in the range of 5.1 ± 0.7 nm (average on 50 measurements). This value is close to that of SiO_2 particles (4.1 ± 1.3 nm and 6.7 ± 2 nm for unmodified and modified nanoparticles, respectively). Thus MPTS-modified SiO_2 used as PMMA's crosslinker allows elaborating nanoscale dispersed hybrid materials.

Second, the methacrylate function number on nanoparticles surface that involves during MMA polymerization have been evaluated. To this end, the molecular weight between crosslinks (Mc) has been determined by swelling of the PMMAx-SiO_2 networks with dichloromethane (Table 2). Indeed, dichloromethane is a PMMA good solvent since it has a solubility parameter ($\delta_{CH_2Cl_2}$ = 20.2 $MPA^{1/2}$) close to that of PMMA (δ_{PMMA} = 19.4 $MPA^{1/2}$) [28]. The maximum uptake decreases from 320 to 270% when the SiO2 nanoparticle proportion increases from 4.5 to 7 wt%, with evidence of a cross-linking density increase. The theoretical weight Mc of PMMAx-SiO2 networks was d calculated with the Flory and Rehner equation [29] (Eq.4.):

$$Mc = \frac{V_1 \rho_2 [(v_2/2) - v_2^{1/3}]}{Ln(1-v_2) + v_2 + \chi_{12} v_2^{2}} \qquad \text{Equation 4}$$

where V_1 is molar fraction of CH_2Cl_2 (63.9 $L.mol^{-1}$) [30], ρ_2 the PMMA density (1.18 $g.cm^{-3}$), υ_2 the polymer volume fraction, and χ_{12} the interaction parameter PMMA / CH_2Cl_2 set at 0.34 [31].

x (wt%)	4.5	6	7
Uptake (%)	320	260	270
Experimental Mc ($g.mol^{-1}$)	2100	1500	1550
Theorical Mc ($g.mol^{-1}$)	250	180	150

Table 2. Uptake in dichloromethane and experimental and theoretical molecular weights between crosslinks (Mc) of PMMAx-SiO_2 networks.

The estimated molecular weight between crosslinks (Mc) decreases from 2100 to 1500 when the nanoparticles proportion increases. Parallelly, the theoretical weight Mc has been calculated from the number of MPTS grafted on silica surface by assuming a homogeneous distribution in the material and a total polymerization of methacrylate functions. The theoretical Mc is about 10 times lower than the experimental Mc value, i.e. only about 10 mol% methacrylate functions on the nanoparticle surface would be involved in PMMA crosslinking. However, the Flory-Rehner relationship is valid for loosely cross-linked networks in which the size and thus volume fraction of the cross-linker is negligible. This is not the case with the networks containing multifunctional silica cross-linkers. Therefore, the data of experimental Mc and methacrylate functions taking part in the cross-linking process are most likely far from the real values, and thus, these data should be considered as rough estimates. Nevertheless, these results confirm that the nanoparticles act as PMMA's crosslinker.

The cross-linking density of PMMAx-SiO_2 networks was then studied by DMA measurements. Indeed, higher the crosslinking density, higher the mechanical

relaxation temperature of the material and higher the storage modulus at rubbery plateau [6]. Storage moduli (E') and loss factor (tanδ) of the PMMAx-SiO_2 networks were reported versus as a function of temperature in Fig. 5.

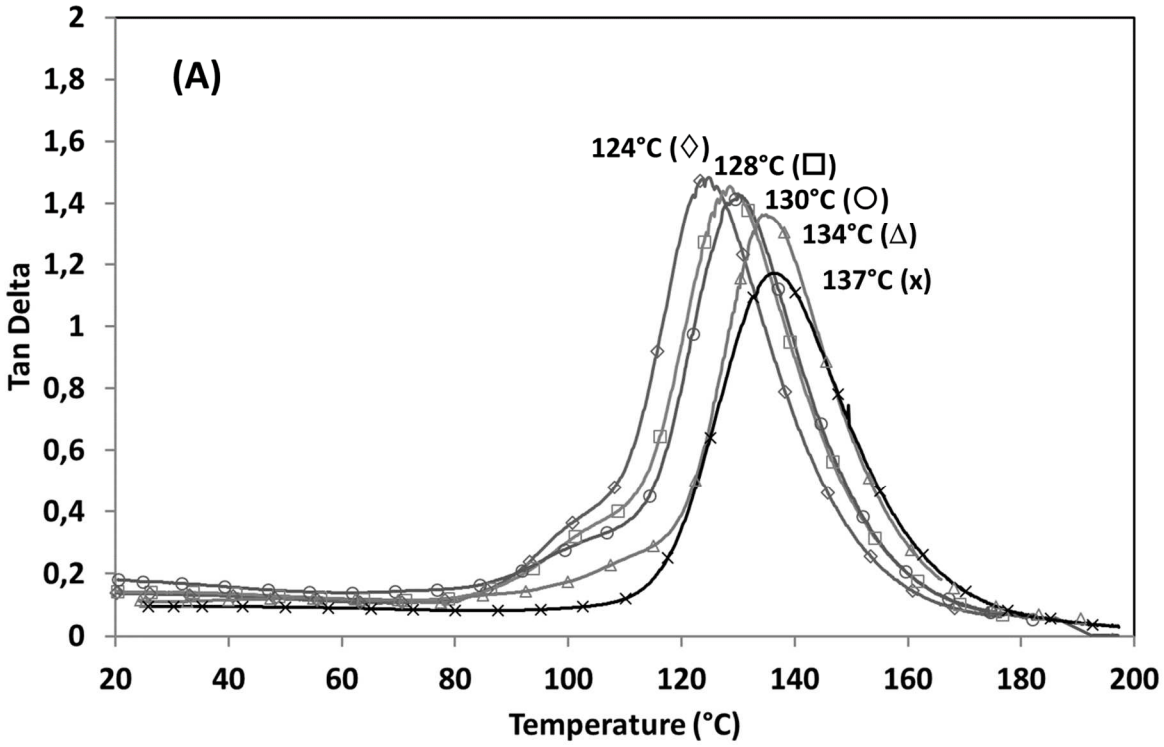

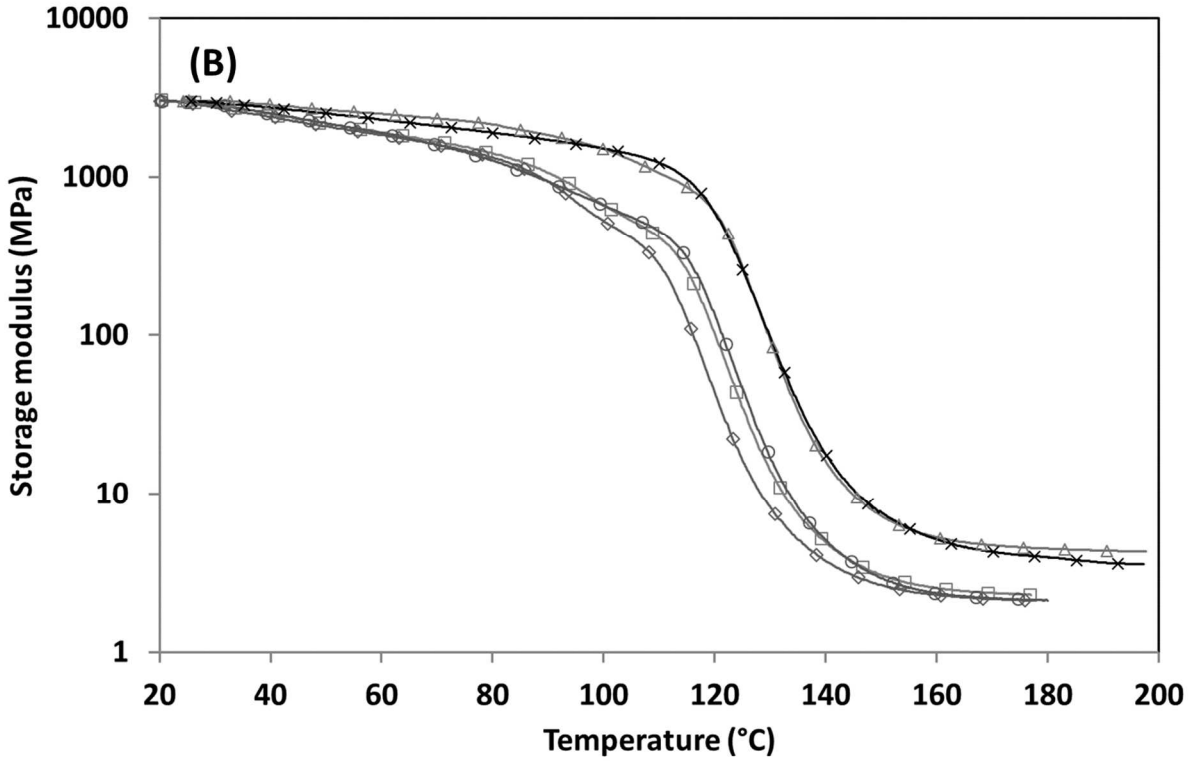

Fig.5. (A) Loss factor and (B) Storage modulus as a function of temperature of $PMMA_x$-SiO_2 networks with x=4.5% (◊), 6% (□), 7% (○), 8.5% (Δ) and 13% (x).

A main α-mechanical relaxation was detected whatever the nanoparticles amount. Its temperature (Tα) increases from 124 to 137° C and the tanδ peak intensity decreases of about 0.4 when the MPTS-SiO_2 nanoparticles proportion increases from 4.5 to 13.5 wt% (Fig.5A.). In addition, up to 8.5 wt%, the tanδ peak width becomes thinner that confirms evidence of a more homogeneous crosslinking density. Simultaneously, the storage modulus at the rubbery plateau (above 150°C) increases from 3 to 5 MPa when the amount of nanoparticles increases from 4.5 to 13.5 wt% (Fig.5B.). These results highlights that both density and homogeneity of PMMA's crosslinking increase with the nanoparticle amount in the material.

A β-mechanical relaxation of PMMA related to the rotation side groups is also observed around Tβ=100°C on tanδ-temperature curves [32]. The corresponding tanδ peak (Fig.5A) and storage modulus decrease (Fig.5B) disappear when the amount of MPTS-SiO_2 nanoparticles increases. Thus, the higher the crosslinking density, the lower freedom of movement of its side chains.

All of the results show that the modified silica nanoparticles behave as the PMMA's crosslinker.

Finally, the stability of $PMMA_5$-SiO_2 networks under artificial UV ageing was studied. The UV-visible spectra were recorded at different ageing times and were compared with those recorded on PMMA network in which PMMA was cross-linked with organic EGDMA (Fig.6). No spectral changes were observed for single PMMA network, whether MPTS-SiO_2 nanoparticles are present. This confirms that the presence of nanoparticles does not affect the PMMA stability over time.

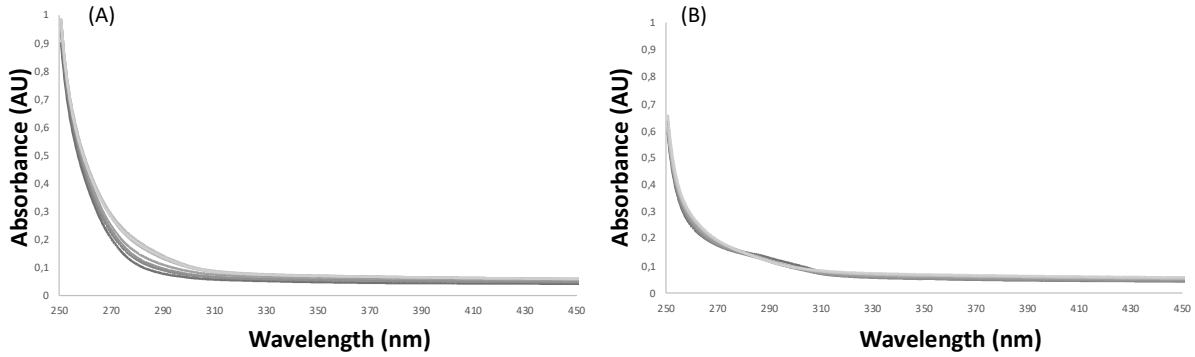

Fig.6. Absorbance of (A) organic $PMMA_5$ network and (B) hybrid $PMMA_5$-SiO_2 network

Thus, the synthesis of transparent PMMA networks can be carried out with silica nanoparticles functionalized with organosilane bearing methacrylate functions as cross-linker. These hybrid $PMMA_x$-SiO_2 networks have been then combined with a PCR39® polycarbonate network in an interpenetrating polymer network (IPN) architecture in order to obtain materials with a better abrasion resistance than single PMMA network or organic PMMA/PCR39® IPNs [6].

3.3. Synthesis and characterization of hybrid $PMMA_x$-SiO_2/PCR39® IPNs:

Hybrid $PMMA_x$-SiO_2/PCR39® IPNs were synthesized from a MMA solution containing MPTS-SiO_2 nanoparticles in which CR39®, DCPD and BPO were added. As CR39® and MMA polymerize according to a free-radical mechanism. their polymerizations were initiated by two initiators decomposing at different temperatures, each being specific to a monomer, in order to limit their copolymerization and the resulting grafting of both networks. Thus DCPD, a low temperature initiator, can initiates the polymerization of reactive MMA at 35°C while a high temperature initiator, BPO (kd = 2.5 × 10 -5 s^{-1}) initiates polymerization of the less reactive CR39® at 80°C [6]. The PCR39®weight proportion ranges from 25 to 75%. It does not need addition of a specific cross-linker because CR39® is tetrafunctional (its homopolymerization leads to a network formation). The thermal cure was set up to 3h at 35°C, 2h at 80°C and a post-cure for 1h at 100°C (Fig.7.). All hybrid $PMMA_x$-SiO_2/PCR39® IPNs are transparent despite the presence of MPTS-SiO_2 nanoparticles (the IPN's transmittance in the visible range is close to 90% except for $PMMA_{13}$-SiO_2/PCR39® (25/75) IPN - close to 80% - Supporting information - Fig.S2.).

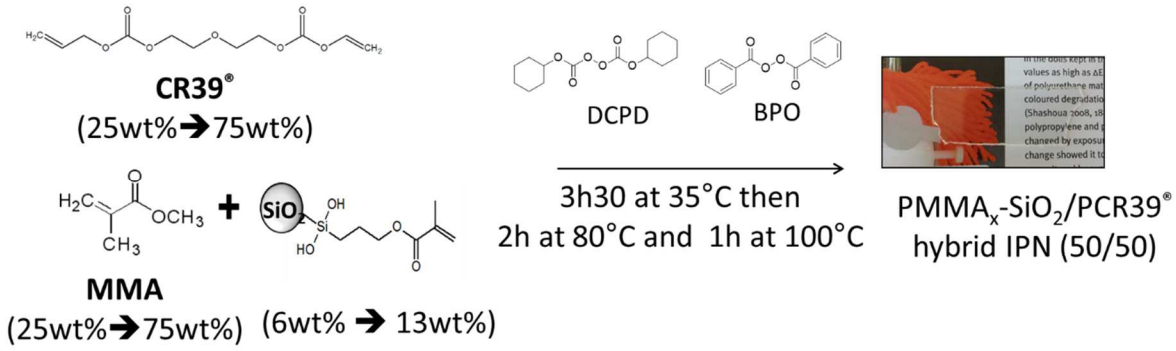

Fig.7. Scheme of hybrid $PMMA_x$-SiO_2/PCR39® IPN synthesis.

All hybrid $PMMA_x$-SiO_2/PCR39® IPNs contain no soluble fraction. PMMA and PCR39® are thus successfully crosslinked inside the IPN architecture. The IPN's synthesis being carried out by mixing all the precursors, the methacrylate functions on the nanoparticle surface copolymerize with the MMA but also possibly with the CR39's allyl functions (this assumption is however unlikely under the used experimental conditions [6]). To verify that SiO_2-nanoparticles mainly crosslink PMMA as in PMMAx-SiO_2 hybrid networks, the storage moduli and loss factors (tanδ) of the hybrid $PMMA_{13}$-SiO_2/PCR39® IPNs were measured and compared with those of the corresponding $PMMA_{linear}$/ PCR39® semi-IPNs in which no MPTS-SiO_2 nanoparticle was inserted (Fig.8.).

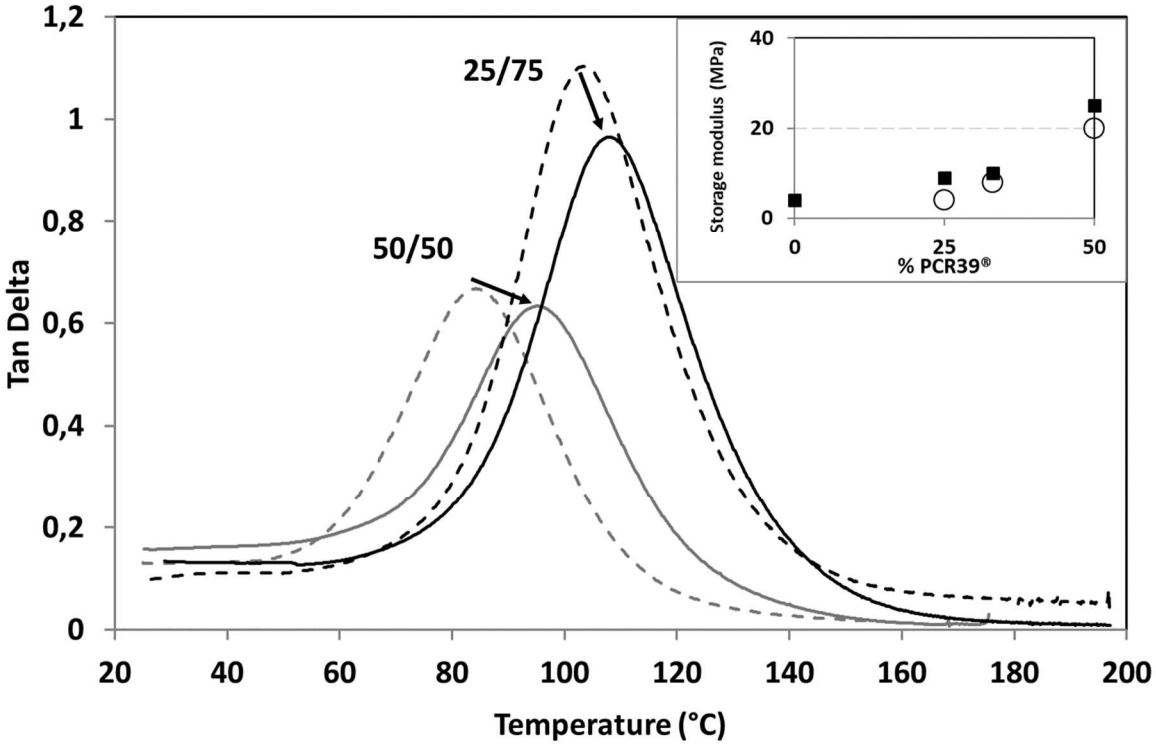

Fig.8. Loss factor of hybrid $PMMA_{13}$-SiO_2/PCR39® IPNs (black line) and of $PMMA_{linear}$/PCR39® semi-IPNs (dashed black line). Insert: Storage modulus at rubbery plateau of hybrid $PMMA_{13}$-SiO_2/PCR39® IPNs (•) and $PMMA_{linear}$/PCR39® semi-IPNs (•).

The hybrid $PMMA_{13}$-SiO_2/PCR39® (50/50) and (25/75) IPNs exhibit higher Tα values than those of corresponding $PMMA_{linear}$/PCR39® (50/50) and (25/75) semi-IPNs. Thus, hybrid $PMMA_{13}$-SiO_2/PCR39® (50/50) IPN shows a relaxation temperature at 96°C against 85°C without nanoparticles. Similarly, the relaxation temperatures were detected at 108°C and 103°C for hybrid $PMMA_{13}$-SiO_2/PCR39® (25/75) IPNs containing or not nanoparticles, respectively. Simultaneously, the storage moduli at the rubbery plateau of hybrid $PMMA_{13}$-SiO_2/PCR39® IPNs are always slightly greater than those of the corresponding $PMMA_{linear}$/PCR39® semi-IPNs (Fig. 8 insert). In addition, the higher the PMMA proportion in IPNs, the more the differences of the modulus at

the rubbery plateau and of the α-mechanical relaxation temperature between IPNs and semi-IPNs are significant. Therefore, it seems that the MPTS-SiO_2 nanoparticles act mainly as the crosslinker of PMMA in these RIPs. To confirm this result, TEM images were recorded to locate nanoparticles (in PMMA or in PCR39® phase) (Fig.4.). The images show clearly black and white domains. Due to the transmission difference, the clear domains have been assigned to an organic phase (PCR39® or / and PMMA) and the dark domains to the MPTS-SiO_2 nanoparticles. The dispersion of nanoparticles in hybrid $PMMA_7$-SiO_2/PCR39® IPN containing 75 and 50 wt% PMMA (Fig.4b and 4c.), appears to be less homogeneous than in the hybrid $PMMA_7$-SiO_2 network (Fig.4a). The nanoparticles would be more concentrated in some organic domains than in others. In addition, the area of nanoparticle concentrated domains seems decrease with the PMMA amount in IPNs. Thus, the modified nanoparticles would be mainly located in the PMMA phase. Finally, the utilization of those nanoparticles would also an original method to stain one of the phases in an IPN architecture.

The last point of this study is the evaluation of scratch resistance of these IPNs (Fig. 9): the deeper the scratch, the lower the scratch resistance.

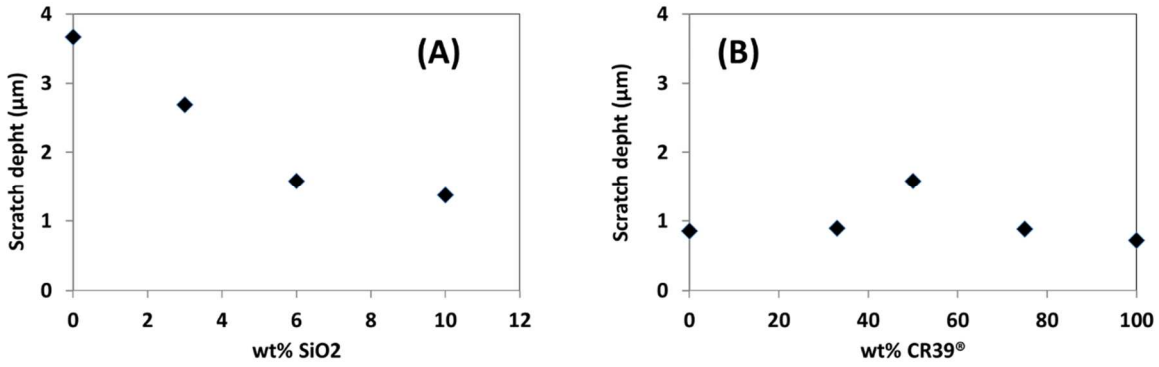

Fig.9. Scratch depth of hybrid $PMMA_x$-SiO_2/PCR39® IPNs as function of (A) MPTS-SiO_2-nanoparticles in $PMMA_x$-SiO_2/PCR39® (50/50) IPN and (B) PCR39® proportion in a hybrid $PMMA_6$-SiO_2/PCR39® IPNs.

As expected, the increase from 0 to 6 wt% MPTS-SiO_2 nanoparticle content in the hybrid $PMMA_x$-SiO_2/PCR39® (50/50) IPN induces a decrease of the scratch depth from 3.7µm to around 1.5µm (Fig.9A). Beyond 6 wt% MPTS-SiO_2 nanoparticles content, the scratch depth remains the same. Thus, the scratch depths on the hybrid IPNs are twice lower than those carried out on the organic $PMMA_{linear}$/PCR39® IPNs. This result is in agreement with the fact that generally the addition of inorganic fillers addition significantly increases the material hardness which is directly related to anti-scratch properties [9]. In order to identify which of PCR39® or SiO_2-nanoparticles has an overriding effect on the scratch resistance, the scratch depth has also been measured as a function of the PCR39® proportion at 6 wt% nanoparticle proportion (with respect to PMMA). While the PCR39® proportion was varied from 25 to 75 wt%, the scratch depth seems constant around 0.8 µm (Fig.9B). Thus, despite their dilution, the SiO_2-nanoparticle effect on the scratch resistance of the IPNs is greater than that of PCR39®.

4. Conclusion

While most of the hybrid interpenetrating polymer networks reported in literature are synthesized by elaborating the inorganic phase by an in-situ sol-gel reaction, we have shown that modified-SiO_2 nanoparticles can be also directly included in PMMA phase

and be evenly distributed inside. To this end, SiO_2 nanoparticles must be previously modified with methacrylate functions which simultaneously allow a correct dispersion in MMA monomer and being the PMMA cross-linker. To assure material's transparency, silica less than 10 nm diameter has been chosen and previously modified. First, single PMMA networks have been synthesized with various modified SiO_2-nanoparticles amounts. The PMMA cross-linking has been checked by solid-liquid extraction and DMA analysis. The dispersion of nanoparticles has been also checked by TEM microscopy and TGA analysis. These hybrid PMMA network have been then associated to polycarbonate network inside an IPN architecture. While IPNs are synthesized according to an in-situ synthesis, nanoparticles are mainly located in PMMA phase. As expected, transparency (transmittance higher than 80%) is kept and, finally, the addition of only 3 wt% of nanoparticles provides improved scratch resistance (hybrid IPN's scratch depth is twice lower than those of the simple PMMA network and of the organic PMMA/PCR39® IPN). This study has therefore opened a new way for the preparation of IPNs hybrid. It is possible to consider changing the nature of nanoparticles to provide additional properties to the materials as photo-luminescency.

Acknowledgements

We gratefully thank the Fondation des Sciences du Patrimoine for financing Mickaël Berrebi 's research grant (ANR-10-LABX-0094-01 – Reference: EUR-17-EURE-0021).

Data availability:

The raw/processed data required to reproduce these findings cannot be shared at this time due to technical or time limitations.

References

[1] J. Brandrup, EH. Immergut, EA. Grulke, Polymer Handbook, 4th ed., Wiley, New York,1999.

[2] E. Snitzer, Optical maser action of Nd^{3+} in a barium crown glass, Phys. Rev. Lett. 7(1961) 444-446.

[3] BJ. Briscoe, PD. Evans, SK. Biswas, SK. Sinha, An experimental study of the nano-scratch behaviour of poly (methylmethacrylate), Tribol. Int. 29 (1996) 93-104.

[4] H. Pelletier, AL. Durier, C. Gauthier, R. Schirrer, Viscoelastic and elastic-plastic behaviors of amorphous polymeric surfaces during scratch, Tribol. Int. 41 (2008) 975-984.

[5] LH. Sperling, D. Klemper, LA. Utracki, Interpenetrating polymer networks, American Chemical Society, Washington, 1991.

[6] M. Berrebi, I. Fabre-Francke, B. Lavédrine, O. Fichet, Development of organic glass using Interpenetrating Polymer Networks with enhanced resistance towards scratches and solvents, European Polymer Journal 63 (2015) 132-140.

[7] F. Bauer, V. Sauerland, H. Glasel, H. Ernst, M. Findeisen, E. Hartman, H. Langguth, B. Marquardt, R. Mehnert, Preparation of scratch and abrasion resistant polymeric nanocomposites by monomer grafting onto nanoparticles, 3ª Effect of filler particles and grafting agents, Macromol. Mater. Eng. 287 (2002) 546-552.

[8] H. Gläsel, F. Bauer, H. Ernst, M. Findeisen, E. Hartman, H. Langguth, R. Mehnert, R. Schubert, Preparation of scratch and abrasion resistant polymeric nanocomposites by monomer grafting onto nanoparticles, 2-characterization of radiation-cured polymeric nanocomposites, Macromol. Chem. Phys. 201 (2000) 2765-2770.

[9] F. Bauer, R. Mehnert, UV Curable Acrylate Nanocomposites: Properties and Applications, J. Polym.Res. 12 (2005) 483-191.

[10] MW. Ellsworth, MN. Bruce, Mutually interpenetrating inorganic-organic networks. New routes into nonshrinking sol-gel composite materials, J. Am. Chem. Soc. 113 (1991) 2756 -2758.

[11] AEJ. Pope, M. Asami, JD. Mackenzie, Transparent silica gel–PMMA composites, J. Mater. Res. 4 (1989) 1018-1026.

[12] SM. Khaled, R. Sui, PA. Charpentier, AS. Rizkalla, Synthesis of TiO_2–PMMA Nanocomposite: Using Methacrylic Acid as a Coupling Agent, Langmuir 23 (2007) 3988-3995.

[13] T. Otsuka, Y. Chujo, Poly(methyl methacrylate) (PMMA)-based hybrid materials with reactive zirconium oxide nanocrystals, Polymer Journal 42 (2010) 58-65.

[14] Y. Liu, C. Hsu, KY. Hsu, Poly(methylmethacrylate)-silica nanocomposites films from surface-functionalized silica nanoparticles, Polymer 46 (2005) 1851-1856.

[15] PS. Chinthamanipeta, S. Kobukata, H. Nakata, D. Shipp, Synthesis of poly(methyl methacrylate)–silica nanocomposites using methacrylate-functionalized silica nanoparticles and RAFT polymerization, Polymer 49 (2008) 5636-5642.

[16] M. Avella, M. Errico, E. Martuscelli, Novel PMMA/$CaCO_3$ nanocomposites abrasion resistant prepared by an in situ polymerization process, Nano Lett. 1 (2001) 213-217.

[17] R. Rodriguez, M. Estevez, S. Vargas, A. Modragon, Hybrid ceramic-polymer material for wood coating with high wearing resistance, Mater Res Inn. 7 (2003) 80-84.

[18] FJ. Carrion, J. Sanes, MD. Bermudez, Influence of ZnO nanoparticle filler on the properties and wear resistance of polycarbonate, Wear 262 (2007) 1504-1510

[19] MD. Bermúdez, W. Brostow, FJ. Carrión-Vilches, J. Sanes, Scratch resistance of polycarbonate containing ZnO nanoparticles: effects of sliding direction, J. Nanosci. Nanotechnol. 10 (2010) 6683-6689.

[20] Z. Wang, G. Xie, X. Wang, G. Li, Z. Zhang, Rheology enhancement of polycarbonate/calcium carbonate nanocomposites prepared by melt-compounding, Mat. Lett. 60 (2006) 1035-1038.

[21] HR. Hakimelahi, I. Hu, IBB.Rupp, MR. Coleman, Synthesis and characterization of transparent alumina reinforced polycarbonate nanocomposite, Polymer 51 (2010) 2494-2502.

[22] ZZ. Wang, P. Gu, Z. Zhang, Indentation and scratch behavior of nano-SiO_2/polycarbonate composite coating at the micro/nano-scale, Wear 269 (2010) 21-25.

[23] A. Lungu, NM. Florea, CM. Damian, H. Iovu, Thermo-mechanical properties of interpenetrating polymer networks (IPNS) filled with fumed silica nanoparticles, Materiale Plastice 3 (2011) 209-213.

[24] R. Mueller, HK. Kammler, K. Wegner, SE. Pratsinis, H surface density of SiO_2 and TiO_2 by thermogravimetric analysis, Langmuir 19 (2003)160-165.

[25] ZW. Wang, TJ. Wang, ZW. Wang, Y. Jin, The adsorption and reaction of a titanate coupling reagent on the surfaces of different nanoparticles in supercritical CO 2, Journal of Colloid and Interface Science 304 (2006) 152-159.

[26] C. Bartholome, E. Beyou, E. Bourgeat-Lami, P. Chaumont, N. Zydowicz, Nitroxide-mediated polymerization of styrene initiated from the surface of fumed silica. Comparison of two synthetic routes, Polymer 46 (2005) 8502-8510.

[27] F. Bauer, V. Sauerland, H. Ernst, H. Gläsel, S. Naumov, R. Mehnert, Preparation of Scratch- and Abrasion-Resistant Polymeric Nanocomposites by Monomer Grafting onto Nanoparticles, Macromol.Chem.Phys. 204 (2003) 375-383

[28] AFM. Barton, Handbooks of solubility parameters and other cohesion parameters, 2nd ed., CRC Press, Boca Raton, 1991.

[29] H. Lange, Determination of the degree of swelling and crosslinking of extremely small polymer gel quantities by analytical ultracentrifugation, Colloid & Polymer Sci. 264 (1986) 488-493.

[30] CH. Hansen, Hansen Solubility Parameters: A user's Handbook, 2nd Ed., CRC Press, Boca Raton, 2007.

[31] JH. Hildebrand, RL. Scott, The Solubility of Nonelectrolytes, Reinhold Publishing Corporation, New York, 1950.

[32] K. Fukao, S. Uno, Y. Miyamoto, A. Hoshino, H. Miyaji, Dynamics of α and β processes in thin polymer films: Poly(vinyl acetate) and poly(methyl methacrylate), Phys.Rev. 64 (2001) 051807.

Supporting information:

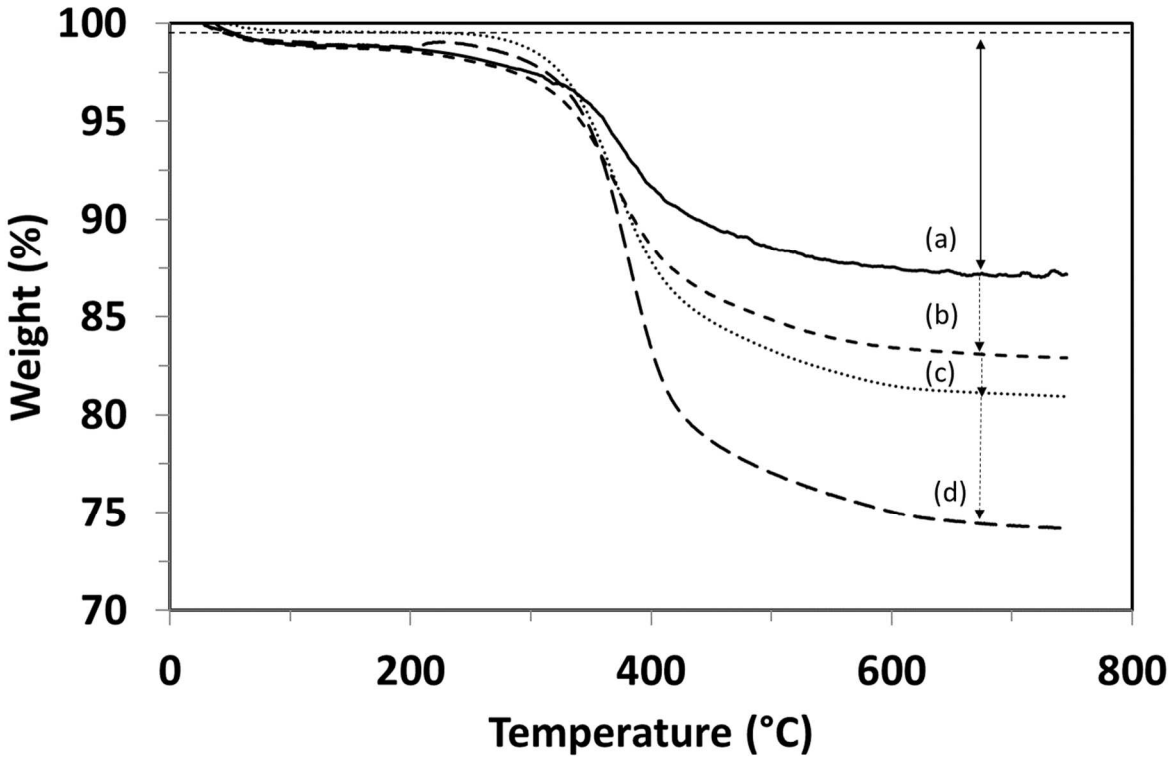

Fig. S1. Thermogravimetric analysis of SiO_2 nanoparticles (……), and MPTS-SiO_2 nanoparticles modified with molar ratio R = 50 (a), 75 (b), 100 (c), 150(d)

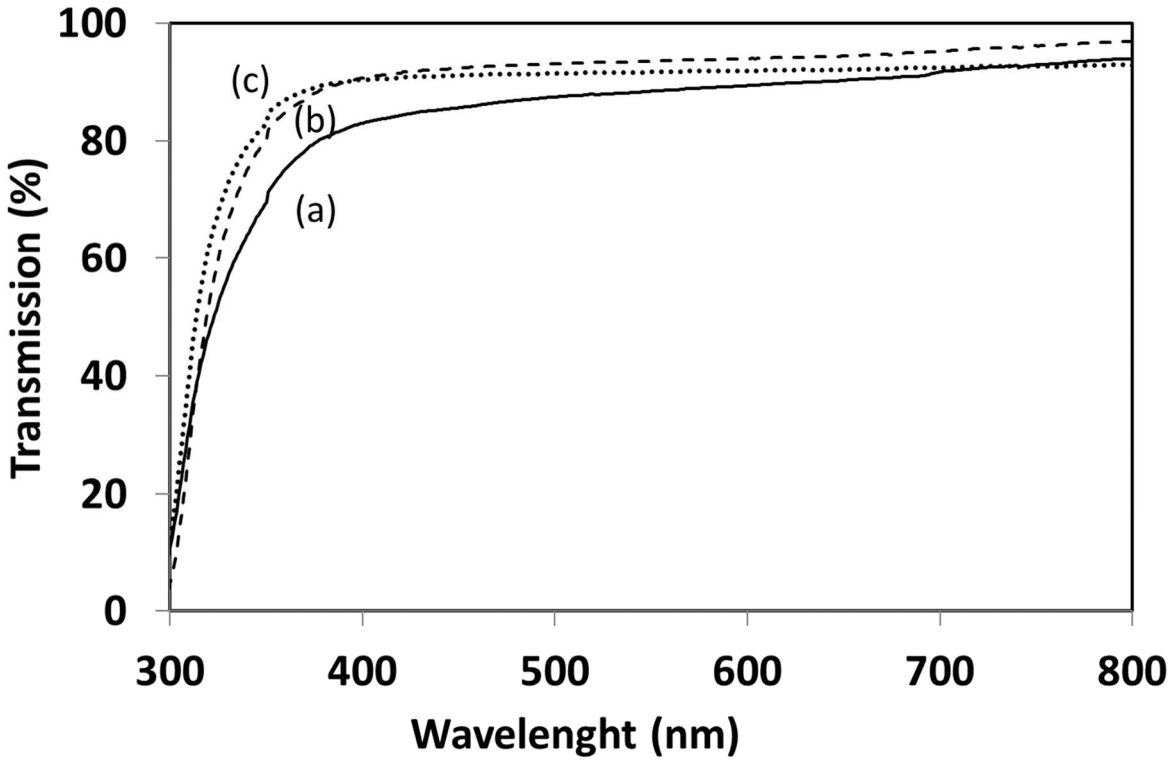

Fig.S2. Transmittance of hybrid $PMMA_{13}$-SiO_2 /PCR39® (a) (25/75), (b) (50-50) and (c) (75-25) IPNs.

Hybrid PMMA combined with Polycarbonate inside interpenetrating polymer network architecture for development of new anti-scratch glass

Isabelle Fabre-Francke, Mickaël Berrebi, Bertrand Lavédrine, Odile Fichet

Transparent and anti-scratch Hybrid PMMA-SiO_2 / PC Interpenetrating Polymer Network